Solid Freeform Fabrication 2019: Proceedings of the 30th Annual International Solid Freeform Fabrication Symposium – An Additive Manufacturing Conference
Reviewed Paper

A Low-Cost Approach for Characterizing Melt Flow Properties of Filaments Used in Fused Filament Fabrication Additive Manufacturing

Jingdong Chen* and Douglas E. Smith*

Department of Mechanical Engineering, Baylor University, 1301 S University Parks Dr, Waco, TX, 76798

Abstract

Users of Fused Filament Fabrication (FFF) can choose from a wide variety of new materials as filament producers continue to introduce new polymer and polymer composite filament into the marketplace. This paper describes a low-cost device capable of measuring the rheological properties of off-the-shelf polymer filament. In this approach, measurements are taken during filament extrusion which are combined with a pressure drop model based on simple shear flow within the FFF nozzle to perform inverse analysis that computes parameters for the power law generalized Newtonian fluid (GNF) model. The applicability of our FFF-filament rheometer is demonstrated with four commercially available polymer filaments by comparing the results to those obtained from a commercial rotational rheometer. A filament characterization approach similar to Melt Flow Index (MFI) is also proposed to assess the extrusion characteristics of materials specific to FFF.

Introduction

Fused Filament Fabrication (FFF) as one of the Additive Manufacturing (AM) techniques shows the enormous potential to benefit the household customers and the professionals in both research and industry due to its cost-effectiveness as well as the wide support from many open source communities. FFF is a molten polymer extrusion-based deposition AM process where a filament of polymer or polymer composite is supplied continuously into a heated liquefier, melted, and then extruded onto the platform or the extrudate below. The gantry system moves the extruder, or in some designs, the build surface to build the product layer-by-layer. [1]

Gaining a thorough understanding of polymer melt rheology behavior in FFF will benefit the processing control as well as the quality of products. Rheological properties of polymer melt, such as the shear-thinning and viscoelasticity govern the flow behavior during processing. Lab scale rheometers which perform off-line measurements can provide various high-quality rheological data of materials. However, common lab scale rheometers cannot incorporate filament directly and instead require the user to first prepare samples of materials for testing. Also, the rheometers are expensive, particular for those who simply want to characterize a filament or measure the fundamental rheological properties of a polymer being considered for FFF before printing. The primary goal of this paper is to develop a new approach for evaluating the rheology of polymers directly from filaments used in FFF.

The flow of polymer melt in FFF may be characterized as pressure-driven flow. Therefore, measuring the pressure drop as the filament is processed through the FFF nozzle provides a means for obtaining rheological properties of materials from an FFF-based device. However, measuring the pressure of the flow in an FFF nozzle has practical difficulties where the small size of nozzle

makes it impractical to attach a pressure gauge inside without having an impact on the flow behavior. Therefore, an indirect pressure measurement method offers promise and will be investigated in this paper.

Several research groups proposed different approaches to monitor the pressure drop of FFF nozzle flow. Phan, et al. [2] measured the consumption of the electric power supplied on the stepper motor used to deliver the filament then converted measured results to the overall pressure drop through the nozzle as a user-defined function of the feedstock feeding rate. Instead of measuring the pressure drop implicitly via the working power of stepper motor , Coogan, et al. [3] and Anderegg, et al. [4] customized the nozzle by inserting a load sensing probe and a piezo-resistive pressure transducer, respectively, into the upper region of the nozzle to measure polymer melt pressure. Our approach differs in that, we developed a relatively simple and low-cost device to obtain pressure drop by directly measuring the extrusion force acting on the filament without interfering the flow inside of nozzle.

The inside geometry of a typical nozzle used in FFF can be recognized as having three regions as shown in **Figure 1**. Region II is a coni-cylindrical region designed to act as a transition zone allowing the polymer melt to accelerate into the capillary die (Region III) such that the shear rate increases significantly, decreasing the shear viscosity while aligned molecular chains without vortex generation. Bellini, et al. [5] assumed a power law generalized Newtonian fluid (GNF) flow in the nozzle with simple shear flow while ignoring entrance and exit effects. In the Bellini model, the total pressure drop in the nozzle is regarded as the sum of the pressure drops from each of the three regions in **Figure 1**. This model is commonly used in FFF analysis such as the work conducted by Ramanath, et al. [6], Sukindar, et al. [7], Pandey, et al. [8], and Tlegenov, et al. [9], and its feasibility as describing the polymer melt flow behavior in FFF is supported by these works. In this paper, we employed this model to predict the pressure drop contribution from the three separate regions and then use the computed pressure drop data to obtain rheological data.

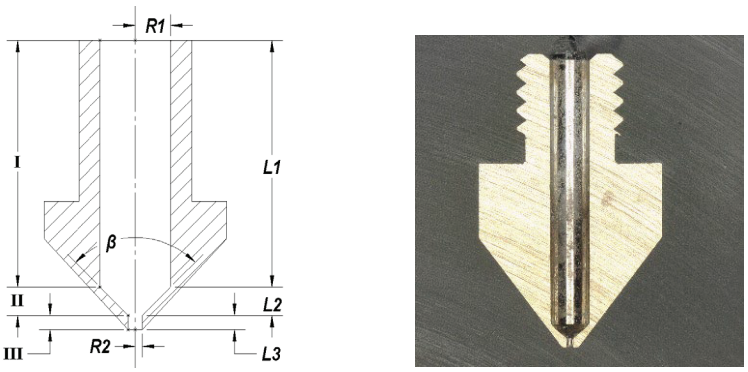

Figure 1. (a) Sketch of the typical inside geometry of a nozzle used in FFF that consists of three regions: I, upper cylindrical die; II, coni-cylindrical die; III, capillary die. (b) Cross-sectional view of the nozzle used in this study

Experimental Methods

Materials

Before describing our device for measuring filament rheological properties it is helpful to note that this study included measurements with commercially available filaments. Four neat polymers were considered in this study which includes two brands of ABS (3DXTECH and Triptech Plastic), PLA (3DXTECH), and Amphora (Triptech Plastic) in filaments with 1.75 mm diameter. The

rheological properties of all materials were obtained using the HAAKE MARS 40 (Thermo Fisher Scientific, Waltham, MA) cone and plate rheometer. The extreme frequency window set as 0.1–100 Hz for two ABS filaments and 0.5-100 Hz for PLA and Amphora to guarantee the measurements under the linear viscoelastic region (LVER). The oscillation frequency sweep measurements were repeatedly conducted five times for each material. Typical values for dynamic viscosity as a function of oscillation frequency appears in the plot in **Figure 2**. If Cox-Merz rule [10] assumed, then the results could also represent the shear rate dependent viscosity.

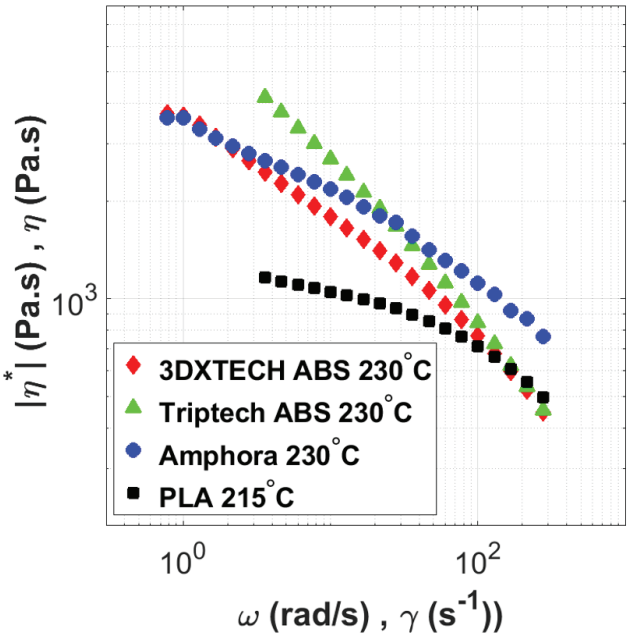

Figure 2. Complex viscosity curves for four neat polymers measured using MARS 40 rotational rheometer.

Device Overview

By separating the liquefier and the stepper motor of a direct extruder system, the overall force acting on the nozzle can be measured via a load cell which is the same as the compressive force in the filament. Assuming the pressure at the nozzle exit is zero, then the measured force recorded by the load cell may be written in terms of the pressure drop ΔP over the entire nozzle as

$$F_f = \Delta P A \tag{1}$$

where A is the area of nozzle inlet and F_f is the resultant force. Our device is composed of an off-the-shelf beam-style load cell along with commercially available FFF machine (or desktop 3D printers) components as shown in **Figure 3**. In this approach, the heated nozzle is separated from the drive system and mounted on the load cell as shown where care is given to ensure that the filament is appropriately aligned with the nozzle axis. Furthermore, assuming that melting only occurs in the nozzle, the measured force equates to the compressive load in the filament between the drive system and nozzle.

Accurate temperature control is required to obtain consistent melt flow measurements. To this end, we use an NTC thermistor along with a K-type thermocouple to monitor the temperature simultaneously where the heater block is redesigned to ensure the two temperature sensors are equal-distanced from the nozzle screw inside the heater block. Generally, the built-in framework of a commercial desktop 3D printer monitors the temperature by interpolating the pre-defined

temperature-resistance table for a certain thermistor. However, we observed significant deviation of temperature readings for these thermistors. Hence, we calibrated the thermistor using ETC-400A (AMETEK Inc, Berwyn, PA) to avoid the deviations, then verified its accuracy using a K-type thermocouple. We also found that the thermocouple had a short delay on reading temperature as compared to the thermistor. Considering the small difference of temperature readings from thermistor and thermocouple along with the difference of their resolution (i.e., 0.01℃ of thermistor and 0.25℃ of thermocouple), the thermistor was selected as the temperature sensor served for our PID controller.

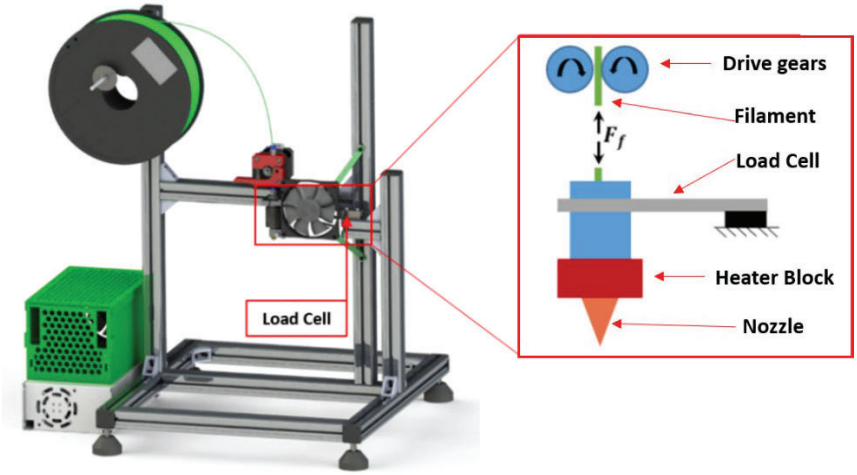

Figure 3. Measuring protocol and design of the FFF filament rheometer

To maintain the desired constant heat flux from the nozzle heater as filament feeding velocity varied, PID control parameters were calibrated for each material under different feeding rate. Then we performed the temperature tests for same material under different delivery speed, and the results show that the maximum temperature fluctuation of the device in operation is about 0.3℃. An example temperature reading appears in **Figure 4**.

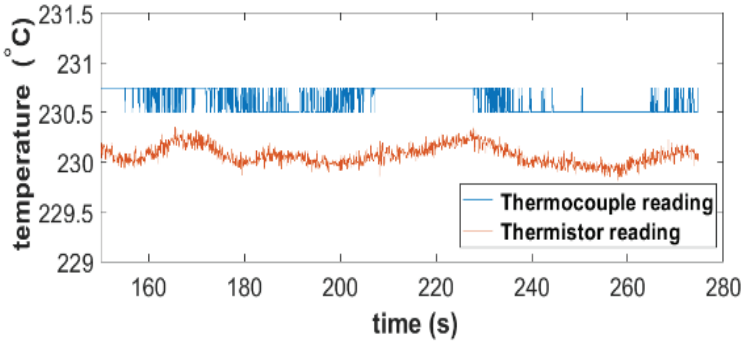

Figure 4. Performance of PID control for 3DXTECH ABS under extrusion at 1.5 RPM 230 ℃.

Considering the temperature effect on viscosity in *equation 2*, we applied the Arrhenius law (*equation 3*) which is valid for temperatures well-above the glass transition to determine the impact from the temperature fluctuation. In these equations, T_0 is the reference temperature, (which is also the setpoint of operation temperature in this case), T is the real-time temperature, $\dot{\gamma}$ is the shear rate, η_0 is the viscosity at T_0, E_0 is the activation energy, and R_g is the gas constant. Using the

activation energy in [11] for PLA and [12] for ABS, we found that the activation energy of the FFF materials assessed in this paper has the magnitude of $10^2\ KJ/mol$. This small fluctuation of temperature yields values of $H(T)$ near to 1 which supports our isothermal assumption.

$$\eta(T,\dot{\gamma}) = H(T)\eta_0(\dot{\gamma}) \tag{2}$$

$$H(T) = exp[\frac{E_0}{R_g}(\frac{1}{T}-\frac{1}{T_0})] \tag{3}$$

Volumetric flow rate of the extrudate for each material under varying filament feeding velocities was obtained by averaging three repeatable measurements. This approach is straightforward but somewhat time-consuming. To simplify the experimental procedure, an alternative approach is considered here by converting the RPM of stepper motor to the volumetric flow rate

$$\bar{v} = \frac{R_e \pi N R_f^2}{30 R_1^2} \tag{4}$$

where N is RPM, R_f is the radius of filament, R_1 is the radius of the inlet of nozzle which is slightly greater than the filaments', R_e is the effective radius of the driving gear. The volumetric flow rate may be written as a function of RPM as

$$Q = \bar{v}(N)\pi R_1^2 \tag{5}$$

Before performing force measurements, rollers and a tension spring which applies a compression force to filament as it passes through the extruder were selected. The compressive force applied by the teeth of the roller must avoid bucking and stripping of filament. Also, the stepper motor was set to provide a precise RPM under 1/32 micro-steps while still being capable of providing sufficient torque. We considered that the filament melt flow in the nozzle can be regarded as nearly steady flow with respect to a well-controlled temperature as well as the smooth and precise filament feeding process. Unfortunately, the load signal appearing in **Figure 5** (a) exhibits a level of variation that is too high for reliable force measurement. Therefore, the force signal is analyzed here to gain a better understanding of fluctuations in the signal.

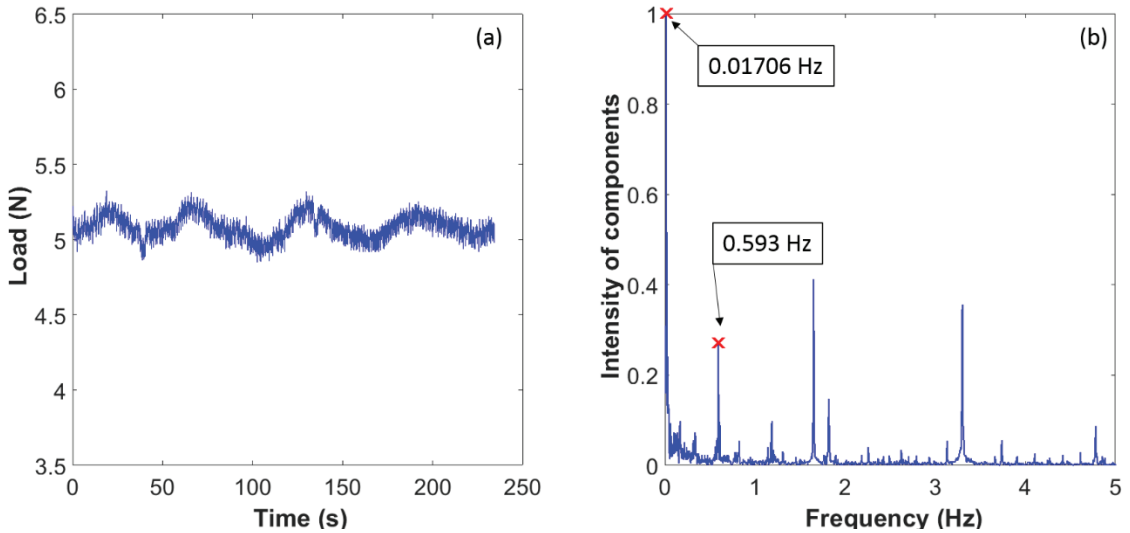

Figure 5. (a), Original force signal of 3DXTECH ABS extruded under 210°C & 1 RPM; (b), One-sided FFF frequency spectrum of the signal.

A one-sided frequency spectrum of the force signal is given in **Figure 5** (b) obtained by performing the Fast Fourier Transform (FFT) where the first dominant frequency component is removed to gain a clear view of other signals. The magnitude of the signal at each frequency was normalized to the scale of one to make it easier to compare the intensity of each frequency component. Two explicit factors causing the fluctuation of the force signal were detected by comparing the data in both time and frequency domain. A frequency peak at 0.01706 Hz was found to be near the rotational frequency (0.0167 HZ) of stepper motor which was operating under 1RPM in this example. Notice that this frequency also matches to the frequency of the repeatable peaks of the signal in time domain (cf. **Figure 5** (a)). This infers that either the idler pulley or the drive gear is not perfectly round, resulting in the filament insertion velocity of the changing over time. Also, the 0.593 Hz bin in FFT plot was found to be equivalent to the 0.6 Hz frequency of the drive gear tooth impact on the filament (i.e., 36-tooth spinning with speed of 1 RPM). Other higher but non-dominant frequency content may be caused by backflow of the molten material as discussed in Gilmer, et al.'s work [13] or the electrical noise from the circuit were filtered by implementing a low-pass filter in Arduino. Once extrusion begins and the initial transient response passes, a PID control maintains the heat flux to be nearly constant such that the temperature and volumetric flow rate remain nearly constant. Therefore, the force measurements were averaged over time where the time window was selected to provide a stable temperature reading to obtain the consistent readings.

Once consistent force readings were obtained, the experiments on our device were performed for each material listed above at various filament feeding speeds from 0.5 RPM to 2.5 RPM drive gear speeds with 0.5 RPM as the increment. At each speed, both pressure drop and volumetric flow rate were obtained and further analyzed. The measured relationship between pressure drop and volumetric flow rate corresponding to each material appears in **Figure 6**.

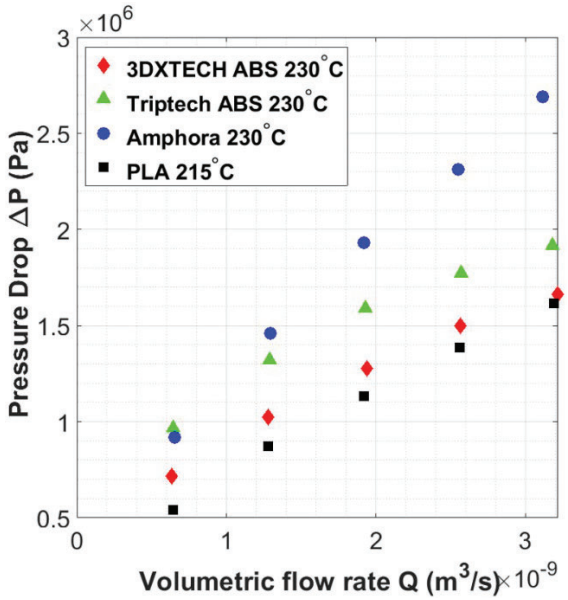

Figure 6. Pressure drop versus volumetric flow rate for four polymers at five filament feeding rate

Results and Analysis

Inverse Analysis

We made several reasonable assumptions to simplify the modeling approach for the complex flow based on Bellini's model [5]. The assumptions with regard to boundary conditions, thermodynamic, flow, and rheological behavior used in this study are given as follows:

1. *Incompressible polymer melt flow;*
2. *No-slip boundary condition at the nozzle wall;*
3. *Isothermal fluid flow condition;*
4. *Gravity of extrudate is negligible;*
5. *Polymer melt flow is in steady state;*
6. *The pressure at the nozzle outlet is equal to zero;*
7. *Flow entrance and exit effects are negligible.*
8. *The melt rheology is purely viscous and can be modeled with as a Generalized Newtonian Fluid.*
9. *The power law model is applicable to polymer melt flow in the nozzle during extrusion.*
10. *The Reynolds number of the flow is small making it possible to ignore inertia effects* [14].
11. *The flow is axisymmetric with respect to the z-axis (cf.* **Figure 1***)*

The purely viscous power law describes the viscosity as a function of strain rate as

$$\eta(\dot{\gamma}) = k\dot{\gamma}^{1-n} \tag{6}$$

where *k* is consistency index and *n* is power law index. The resulting expression for pressure drop in each region of an FFF nozzle based on *equation 6* may be written as given in Bellini as

$$\Delta P_I = 2kL_1\left(\frac{Q(1/n+3)}{\pi R_1^{3+1/n}}\right)^n, \tag{7}$$

$$\Delta P_{II} = \frac{2k\cot\frac{\beta}{2}}{3n}\left(\frac{Q\left(\frac{1}{n}+3\right)}{\pi}\right)^n (R_2^{-3n} - R_1^{-3n}), \tag{8}$$

and

$$\Delta P_{III} = 2kL_3\left(\frac{Q(1/n+3)}{\pi R_2^{3+1/n}}\right)^n \tag{9}$$

where regions I, II, and III are defined in **Figure 1**. The overall pressure drop in an FFF nozzle is computed by summing ΔP_{I}, ΔP_{II}, and ΔP_{III} yielding

$$\Delta P = \Delta P_1 + \Delta P_2 + \Delta P_3 = 2k\left(\frac{Q(\frac{1}{n}+3)}{\pi}\right)^n \left[\frac{L_1}{R_1^{3n+1}} + \frac{\cot\frac{\beta}{2}}{3n}(R_2^{-3n} - R_1^{-3n}) + \frac{L_3}{R_2^{3n+1}}\right] \tag{10}$$

where $R_1, R_2, L_1, L_3,$ and β define the geometry of the nozzle as shown in **Figure 1**(a). Substituting *equation 5* into *equation 10* yields the pressure drop as a function of filament feeding velocity.

The nozzle used in this study appears in **Figure 1** (b). Given that the only unknowns in *equation 10* are the power law parameters n and k, we employed an inverse analysis approach to predict these parameters from the experimental data of ΔP and Q. To this end, a nonlinear least-square curve-fitting method was implemented in MATLAB (MathWorks, Inc., Natick, MA) based on the Gauss-Newton algorithm to fit the measurements of Q and ΔP. In this approach, *n* and *k* are updated iteratively according as

$$\{A\}^{j+1} = \{A\}^j + \left[[Z^j]^T[Z^i]\right]^{-1}\{[Z^j]^T\{D^j\}\} \tag{11}$$

where {A} is a vector of unknown parameters of interest, [Z] is the Jacobian matrix composed of derivatives of ΔP with respect to *n* and *k*, the vector {D} contains the residuals between the

measured pressure drop and those from prediction, and j represents the iteration numbers. The partial derivatives of pressure drop with respect to n and k compose [Z] are

$$\frac{\partial \Delta P}{\partial k} = (L_1 R_1^{-1-3n} + L_3 R_2^{-1-3n} + \frac{\cot\left(\frac{\beta}{2}\right)(-R_1^{-3n}+R_2^{-3n})}{3n}) 2\pi^{-n} \left(3+\frac{1}{n}\right)^n Q_i^n \tag{12}$$

$$\frac{\partial \Delta P}{\partial n} = \frac{-2k\pi^{-n}\left(3+\frac{1}{n}\right)^n Q_i^n R_1^{-3n}}{3(1+3n)} \left\{\frac{3L_1}{R_1}(A + C\,lnR_1\,) + \frac{R_2^{-1-3n}}{n^2}\left[3n^2(A + ClnR_2)L_3 R_1^{3n} + cot\left(\frac{\beta}{2}\right) R_2(B + DlnR_2)R_1^{3n} + (B - DlnR_1)R_2^{3n})\right]\right\} \tag{13}$$

where $A,B,C,$ and D are user-defined functions used to simplify the expression of *equation 13* and are given in the following equations as

$$A = 1 + log(\pi) + 3nln(\pi) - (1+3n)\,log\left(Q\left(3+\frac{1}{n}\right)\right), \tag{14}$$

$$B = 1 + n(4 + log(\pi) + 3nlog(\pi)) - n(1+3n)log\left(\left(3+\frac{1}{n}\right)Q\right), \tag{15}$$

$$C = 3 + 9n\,, \tag{16}$$

and

$$D = 3n(1+3n) \tag{17}$$

The coefficient of determination (r^2) was computed in the usual manner for each material is greater or equal to 0.99 which suggested the math model fits to the experimental data very well. Fitted data appears in **Figure** 7. Values of n and k computed in our inverse analysis along with the corresponding values of r^2 appear in **Table 1**.

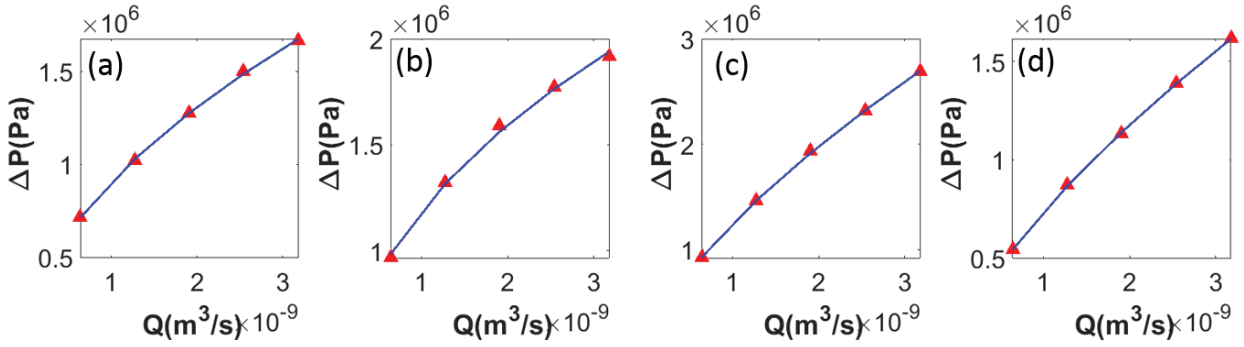

Figure 7. Curve fitting results for: (a), 3DXTECH ABS at 230℃; (b), TRIPTECH ABS at 230℃; (c), Amphora at 230℃; (d), PLA at 215℃, where the red triangle markers are our measurements of pressure drop and the blue solid lines are curve-fitting results.

Table 1. Power law parameters predicted via inverse analysis approach

Filaments	Temperature (℃)	n	k (Pa · s^n)	r^2
ABS (3DXTECH)	230	0.498	6.678e3	0.999
ABS (Triptech Plastic)	230	0.425	1.219e4	0.997
Amphora (Triptech Plastic)	230	0.682	6.221e3	1.000
PLA (3DXTECH)	215	0.681	2.878e3	1.000

Rheology Evaluation

Power law parameters obtained from our inverse analysis may be substituted into *equation 6* to obtain values of computed viscosity as a function of shear rate for each material considered in this study. Assuming Cox-Merz rule, results in **Figure 2** were compared to the predictions using the power law parameters obtained in above inverse analysis, and the comparison appears in **Figure**

8. Here we consider a range of angular frequency (or shear rate) between 50 rad/s to 280 rad/s (or 50 s^{-1} to 280 s^{-1}) since this is the averaged power law apparent wall shear rate in regions *I* and *III* (cf. **Figure 1**(a)) when our filaments are extruded at 0.5RPM-2.5RPM. In addition, a shear rate of 280 rad/s is the maximum angular frequency that can be measured with MARS 40 to guarantee the accuracy. Note that computed values of power law viscosity describe the shear thinning behavior very well for all materials considered here over the shear rate region typical of FFF processing.

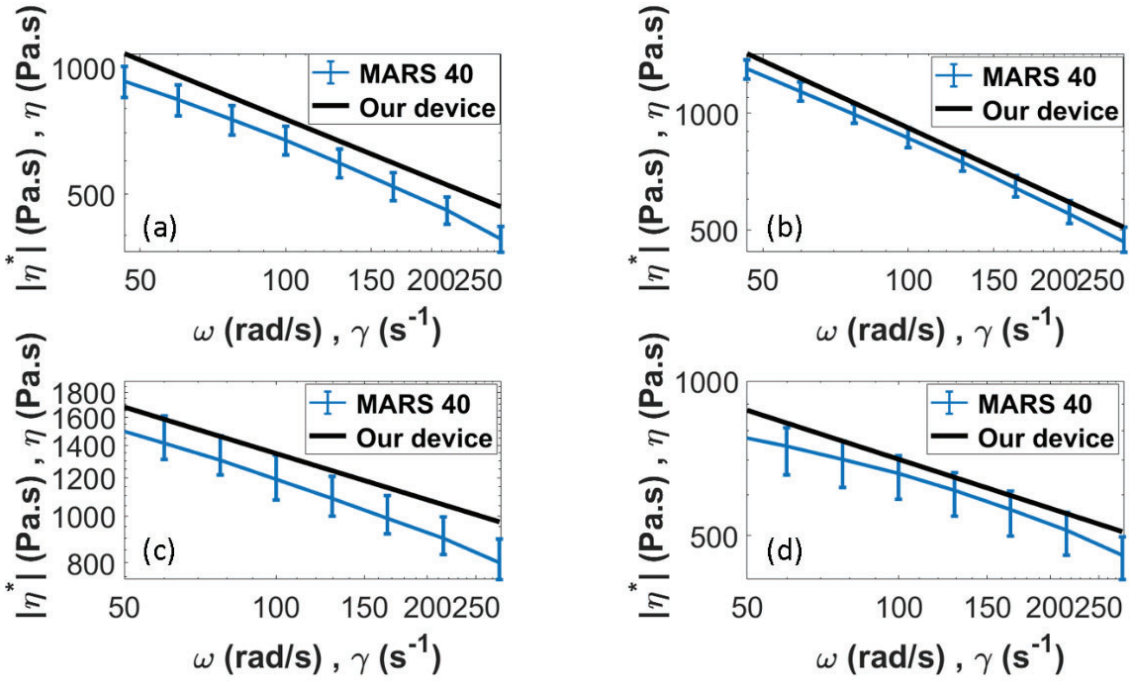

Figure 8. Comparison results of viscosity with respect to the shear rate form 50 s^{-1} to 280 s^{-1} from MARS 40 and our device for (a), 3DXTECH ABS; (b), TRIPTECH ABS; (c), TRIPTECH Amphora; (d), 3DXTECH PLA.

To further compare the power law parameters obtained using our device to those from MARS 40, we employed the same approach as in above inverse analysis, least-square curve fitting, to obtain *n* and *k* from measured viscosity data in **Figure 2**. Note that fitted values of power law parameters from MARS 40 data are sensitive to the shear rate region. Having the above analysis as the premise, power law parameters from MARS 40 are determined over the same shear rate range where values appear in **Table 2** and **3** along with those predicted using our device.

Table 2. Comparison of the power law index (*n*) obtained using our device and those fitted from MARS 40 data

Filaments	**Temperature (℃)**	***n*** Our Device	***n*** MARS 40	**Percentage Error (%)**
ABS (3DXTECH)	230	0.500	0.508	1.6
ABS (Triptech Plastic)	230	0.425	0.418	1.7
Amphora (Triptech Plastic)	230	0.682	0.650	4.9
PLA (3DXTECH)	215	0.681	0.695	2.1

Values in **Table 2** and **3** show that errors are within 6% for both comparison of n and k, and this favorable result suggests that the Bellini model is good for describing the creeping flow in an FFF nozzle, and that our device provides accurate power law data. Even though multiple assumptions have been employed for developing the equation of pressure drop through an FFF nozzle, including the converging flow in region II, the repeatable results for all four polymers demonstrate the validation of our approach of evaluating shear thinning behavior of polymer melt of FFF nozzle flow directly form filaments.

Table 3. Comparison of the power law consistency index (k Pa· s^n) obtained using our device and those fitted from MARS 40 data

Filaments	**Temperature (℃)**	k (Pa · s^n) Our Device	k (Pa · s^n) MARS 40	**Percentage Error (%)**
ABS (3DXTECH)	230	6.678e3	7.043e3	5.2
ABS (Triptech Plastic)	230	1.219e4	1.279e4	4.7
Amphora (Triptech Plastic)	230	6.221e3	5.885e3	5.7
PLA (3DXTECH)	215	2.878e3	3.024e3	4.8

FFF Filament Flow index (FFI)

The Melt Flow Index (MFI) is widely used in the plastics industry that follows either ASTM D1238 [15] or ISO 01133 [16] standards. In the traditional MFI test, under certain temperature and weight of plunger, MFI is defined in units of grams per 10 minutes [15]. Our device is capable of controlling the mass flow rate and measuring the extrusion force, hence we defined a flow index here based on the FFF technology using the extrusion force which we define as a 'Filament Flow Index (FFI)'. The experimental conditions, i.e., processing temperature and speed of stepper motor, were referenced from MakerBot (MakerBot Industries, Brooklyn, NY, USA), a typical desktop-sized FFF machine where 1.2 RPM is a typical feeding rate for the printer as it prints the shell of the part. For each material, 3 measurements were conducted to take the average value. The temperature was selected as the widely applied printing temperature. The resulting FFI is shown in **Figure 9** and **Table 4**.

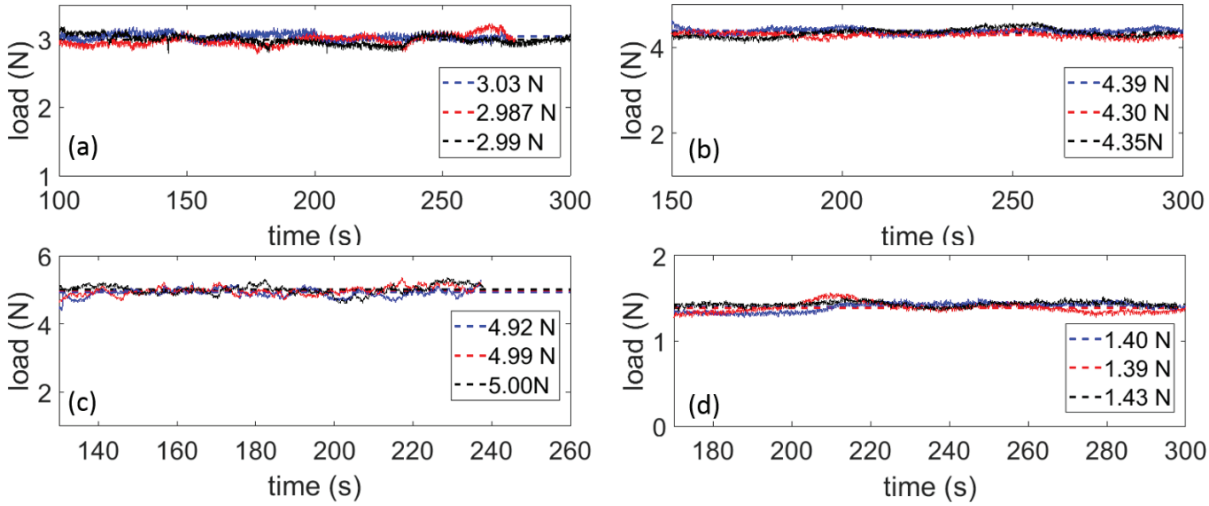

Figure 9. Repeatable FFI measurements for (a), 3DXTECH ABS; (b), TRIPTECH ABS; (c), TRIPTECH Amphora; (d), 3DXTECH PLA, where the dashed lines in each plot represent the average value of the forces.

Our filament flow index (FFI) could provide a measure of fluidity and ease of the polymer melt flow. In our device, the nozzle has a geometrically complex die which does not conform to ASTM D1238. Therefore, when defining an FFI using our device, the value of the force which relates to the processing temperature and filament feeding velocity is used as a processing index analogous to those of MFI for characterizing the FFF filaments.

Table 4 Filament Flow Index - Extrusion force for four polymers materials under the normal processing condition

Parameters	**ABS** (3DXTECH)	**ABS** (Triptech Plastic)	**Amphora** (Triptech Plastic)	**PLA** (3DXTECH)
Stepper Motor Speed (RPM)	1.2	1.2	1.2	1.2
Processing Temperature (℃)	230	230	230	215
Force (N)	3.00	4.35	4.97	1.41

Conclusions

We successfully developed an FFF filament rheometer which is composed of a device and computational approach that directly characterizes the rheological properties of FFF filament. Firstly, a device was fabricated that measures the extrusion force within FFF filament. The extrusion force was used to propose an FFF Filament Melt Index which is analogous to the Melt Flow Index that can quickly provide melt flow information on a filament. Secondly, the pressure drop was measured at a specified temperature at five different volumetric flow rates. This data was used to obtain power law parameters via a Gauss-Newton based inverse analysis. Thirdly, a model for pressure drop model as a function of volumetric flow rate was employed where the polymer melt was assumed to be a lower law flow. The applicability of this model and its merit capable of providing the pressure drop of the FFF nozzle flow was verified.

The accuracy issues of the commercial thermistor used on the FFF printers in the market were detected and solved. The accurate temperature readings acted as the feedback taking into the PID control to guarantee the steady heat flux control adapted to different filament feeding rate for different materials. In addition to the adjustments on temperature, the vibration from start and stop of each step of the stepper motor was minimized by subdividing each step into 32 micro-steps. In addition, the speed of the stepper motor was verified to be accurate and directly related to volumetric flow rate experimentally. All above adjustments benefit the nearly steady state extrusion process resulting in the consistent and repeatable force signal.

Comparison results between the measured viscosities using our device to those obtained with a rotational rheometer shows that both power law index and consistency index can be obtained within 6% error for all polymers. The well-matched results of all four different type of materials demonstrate the feasibility of our approach for evaluating rheology of the both the existing and the new materials in the market. It is also noticed that the two brands of ABS exhibit significantly rheological behavior, and the difference was also detected using our device as presented by both FFI and the power law parameters in **Table 2-4**. In summary, the filament rheometer developed here is shown to be an effective way to quickly characterize the rheology of FFF filaments.

Future Work

Future work includes the investigation of more complex rheology models and the implementation of the device into a stand-alone portable device.

Acknowledgements

The authors would like to acknowledge the financial support offered by Baylor University and many beneficial discussions with Dr. David Jack at Baylor University.

References

1. A. Gold, S., Strong, R., and N. Turner, B., 2014, "A Review of Melt Extrusion Additive Manufacturing Processes: I. Process Design and Modeling," Rapid Prototyp. J., 20(3), pp. 192–204.
2. Phan, D. D., Swain, Z. R., and Mackay, M. E., 2018, "Rheological and Heat Transfer Effects in Fused Filament Fabrication," J. Rheol., 62(5), pp. 1097–1107.
3. Coogan, T. J., and Kazmer, D. O., 2018, "In-Line Rheological Monitoring of Fused Deposition Modeling," J. Rheol., 63(1), pp. 141–155.
4. Anderegg, D. A., Bryant, H. A., Ruffin, D. C., Skrip, S. M., Fallon, J. J., Gilmer, E. L., and Bortner, M. J., 2019, "In-Situ Monitoring of Polymer Flow Temperature and Pressure in Extrusion Based Additive Manufacturing," Addit. Manuf., 26, pp. 76–83.
5. Bellini, A., Güçeri, S., and Bertoldi, M., 2004, "Liquefier Dynamics in Fused Deposition," J. Manuf. Sci. Eng., 126(2), pp. 237–246.
6. Ramanath, H. S., Chua, C. K., Leong, K. F., and Shah, K. D., 2008, "Melt Flow Behaviour of Poly-Epsilon-Caprolactone in Fused Deposition Modelling," J. Mater. Sci. Mater. Med., 19(7), pp. 2541–2550.
7. Sukindar, N. A., Ariffin, M. K. A., Baharudin, B. T. H. T., Jaafar, C. N. A., and Ismail, M. I. S., 2016, "ANALYZING THE EFFECT OF NOZZLE DIAMETER IN FUSED DEPOSITION MODELING FOR EXTRUDING POLYLACTIC ACID USING OPEN SOURCE 3D PRINTING," J. Teknol., 78(10).
8. Pandey, A., and Pradhan, S. K., 2018, "Investigations into Complete Liquefier Dynamics and Optimization of Process Parameters for Fused Deposition Modeling," Mater. Today Proc., 5(5, Part 2), pp. 12940–12955.
9. Tlegenov, Y., Hong, G. S., and Lu, W. F., 2018, "Nozzle Condition Monitoring in 3D Printing," Robot. Comput.-Integr. Manuf., 54, pp. 45–55.
10. Al-Hadithi, T. S. R., Barnes, H. A., and Walters, K., 1992, "The Relationship between the Linear (Oscillatory) and Nonlinear (Steady-State) Flow Properties of a Series of Polymer and Colloidal Systems," Colloid Polym. Sci., 270(1), pp. 40–46.
11. Shojaeiarani, J., Bajwa, D., Rehovsky, C., Bajwa, S., and Vahidi, G., 2019, "Deterioration in the Physico-Mechanical and Thermal Properties of Biopolymers Due to Reprocessing," Polymers, 11, p. 58.
12. Duh, Y.-S., Ho, T.-C., Chen, J.-R., and Kao, C.-S., 2010, "Study on Exothermic Oxidation of Acrylonitrile-Butadiene-Styrene (ABS) Resin Powder with Application to ABS Processing Safety," Polymers, 2(3), pp. 174–187.
13. Gilmer, E. L., Miller, D., Chatham, C. A., Zawaski, C., Fallon, J. J., Pekkanen, A., Long, T. E., Williams, C. B., and Bortner, M. J., 2018, "Model Analysis of Feedstock Behavior in Fused Filament Fabrication: Enabling Rapid Materials Screening," Polymer, 152, pp. 51–61.

14. McIlroy, C., and Olmsted, P. D., 2017, “Deformation of an Amorphous Polymer during the Fused-Filament-Fabrication Method for Additive Manufacturing,” J. Rheol., 61(2), pp. 379–397.
15. ASTM Standard D1238-13 “Standard Test Method for Melt Flow Rates of Thermoplastics by Extrusion Plastometer”. American Society for Testing and Materials International, West Conshohocken, PA. EE.UU.2013
16. ISO 0133-2-2011 “Plastics — Determination of the melt mass-flow rate (MFR) and melt volume-flow rate (MVR) of thermoplastics”